Ab initio giant magnetoresistance and current-induced torques in Cr/Au/Cr multilayers

P. M. Haney,[1,*] D. Waldron,[2,†] R. A. Duine,[3,‡] A. S. Núñez,[4,§] H. Guo,[2,‖] and A. H. MacDonald[1,¶]
[1]*Department of Physics, The University of Texas at Austin, 1 University Station, Austin, Texas 78712, USA*
[2]*Centre for the Physics of Materials and Department of Physics, McGill University, Montreal PQ, Canada H3A 2T8*
[3]*Institute for Theoretical Physics, Utrecht University, Leuvenlaan 4, 3584 CE Utrecht, The Netherlands*
[4]*Instituto de Física, PUCV Avenue Brasil 2950, Valparaíso, Chile*
(Received 18 December 2006; revised manuscript received 16 April 2007; published 21 May 2007)

We report on an *ab initio* study of giant magnetoresistance (GMR) and current-induced torques (CITs) in Cr/Au/Cr trilayers that is based on nonequilibrium Green's functions and spin-density functional theory. We find substantial GMR due primarily to a spin-dependent resonance centered at the Cr/Au interface and predict that the CITs are strong enough to switch the antiferromagnetic order parameter at current densities ~100 times smaller than switching current densities in ferromagnetic metal circuits.

DOI: 10.1103/PhysRevB.75.174428 PACS number(s): 85.75.−d, 71.15.Mb, 72.25.Ba

I. INTRODUCTION

Magnetic metals are often well described using the effective mean-field description provided by the Kohn-Sham equations of spin-density functional theory. In this description, the Kohn-Sham quasiparticles experience exchange-correlation potentials with a spin dependence that is comparable in strength to bandwidths and other characteristic electronic energy scales. The spin-dependent part of the Kohn-Sham quasiparticle potential acts like an effective magnetic field that is locally aligned with the electron spin density. Because of these strong spin-dependent potentials, the resistance of a ferromagnetic metal circuit will change substantially when the magnetization orientation in any part of the circuit is altered, an effect known as giant magnetoresistance (GMR). Conversely, transport currents can destabilize magnetization configurations that are metastable in the absence of a current and change the collective magnetization dynamics. In the case of circuits containing ferromagnetic elements the influence of transport currents on the magnetization can be understood as following from conservation of total spin angular momentum; the torques that reorient quasiparticle spins as they traverse a noncollinear magnetic circuit are accompanied by current-induced reaction torques (CITs) that act on the magnetic condensate. This type of phenomenon is not by any means limited to magnetic systems. For example, there have been recent studies of the interaction between transport and charge density waves (CDWs), which find that the CDW order parameter configuration influences transport and conversely that transport can alter the CDW.[1]

GMR and CITs have been extensively studied, both experimentally and theoretically, in ferromagnetic metal circuits.[2,3] In the case of ferromagnets current-induced torques are generally referred to as spin-transfer torques, since they represent a transfer of conserved total spin angular momentum between the magnetic condensate and quasiparticle currents. The spin-transfer argument is very general but is perhaps a little vague in that it does not always specify what is meant by the magnetic condensate (*magnetization*). (Some work does appeal explicitly to a *s-d* picture of transition metal magnetism with *d*-electron local moments exchange coupled to itinerant *s*-electron bands.)

Several of us have recently proposed[4] that CITs can also act on the order parameter of antiferromagnetic metals. Our proposal follows from a microscopic picture[5] of CITs that applies to a metal with any kind of magnetic order, including antiferromagnetic order, and suggests that CITs are a universal phenomenon in magnetic metals. In this picture CITs arise from the dependence on bias voltage of the relationship between the steady-state Kohn-Sham quasiparticle density matrix and the Kohn-Sham single-particle Hamiltonian. This picture in effect explicitly identifies the energy region between the chemical potentials of source and drain, the transport window, with the transport electrons and the energy region below this with the magnetic condensate. Given the Kohn-Sham Hamiltonian, the condensate contribution to the density matrix can be constructed[6] (for slow condensate dynamics) by solving the time-independent Schrödinger equation for electrons in a system of interest, including, if appropriate, their coupling to electrodes in equilibrium, whereas the transport contribution to the density matrix is constructed by solving the Schrödinger equation with the scattering-theory boundary condition that the electrons be incident from the source. All of this is accomplished conveniently using a nonequilibrium Green's function theory.[6] The change in condensate dynamics, or the current-induced torques, follows from the difference between the Kohn-Sham Hamiltonian constructed from the equilibrium density matrix and the Kohn-Sham Hamiltonian constructed from the density matrix in the presence of a transport voltage. For magnetic condensate dynamics,[6] what is relevant is changes in the spin-dependent parts of the Hamiltonian and, in particular, changes in the direction of the exchange-correlation effective magnetic fields on each site.

Several of us have recently used this approach to explore the possibility of CITs in circuits containing antiferromagnetic metals[4] by studying a simple one-band, Hubbard-interaction, toy model. For this model, we found CITs that drive the antiferromagnetic order parameter which are, remarkably, proportional to film thickness, provided that inelastic scattering[7] is ignored. (In ferromagnets spin-transfer torques saturate at a finite value for large ferromagnetic film thicknesses.) In this paper, we evaluate CITs for a potentially realistic magnetoelectronic system using an *ab initio* non-

equilibrium Green's function (NEGF) formalism.[8] This calculation convincingly demonstrates that GMR and CITs do occur in circuits containing only antiferromagnetic and paramagnetic elements, and that they can be large. The *ab initio* approach accounts for all electronic structure details of the materials and the interfacial bonding between materials, while the NEGF formalism enables the calculation of finite bias properties, such as current, and nonequilibrium spin densities. The specific calculations we report on in this paper were performed on a system with antiferromagnetic (100)-growth-direction bcc chromium (Cr) leads separated by a fcc gold (Au) spacer. The Cr(100)/Au(100)/Cr(100) trilayer system we consider here appears to be attractive as a model system for antiferromagnetic metal spintronics. Au/Cr multilayers and (100)-growth-direction epitaxy were studied some time ago both experimentally[9] and theoretically,[10,11] motivated in part by superconductivity that can occur in disordered Au/Cr films. We find that both GMR and CITs do occur in this ferromagnet-free magnetoelectronic circuit, as anticipated by previous work.[4] Our calculations also identify new physics not anticipated in the early toy-model study. The new features are associated with spin-polarized interface resonance at the Au/Cr interface and with the presence of more than one propagating Cr channel at the Fermi energy for some transverse wave vectors. The paper is organized as follows: in Sec. II, we briefly review our calculation method, while in Sec. III, we give specific details of the system under consideration. We explain our results in Sec. IV, and finally, in Sec. V we present our conclusions and suggest some possible directions for future research directed toward exploring the potential of spintronics in Au/Cr and related systems.

II. METHOD

To calculate equilibrium and nonequilibrium properties of the system, we employ the NEGF formalism within the density functional theory (DFT) framework.[12] The central object in this formalism is the equal-time lesser Green's function, defined as $G^{<}_{j,j'}(t,t) \equiv i\langle c^{\dagger}_{j'}(t)c_j(t)\rangle$. Here the labels j and j' refer to the single-particle basis set in which the nonequilibrium density matrix is evaluated. In the NEGF-DFT formalism one of the labels must specify an atomic site and the other labels specify the spin included and the orbitals included at each site [the density functional theory calculation is carried out with a linear combination of atomic orbitals (LCAO) basis, within the local spin-density approximation (LSDA)]. These calculations normally assume transverse periodicity, either on an atomic scale, as in this calculation, or in the context of a transverse super cell model for transport through a system with a finite cross section. The single-particle basis therefore also includes a transverse wave-vector label. The NEGF formalism implementation employed here has been described in detail in previous work.[12] In the present work we assume that the time dependence of the mean-field Hamiltonian, which is associated with slow condensate dynamics when present, can always be ignored in using the formalism to calculate a steady-state value of $G^{<}_{j,j'}(t,t)$. This steady-state Green's function specifies the nonequilibrium density matrix ρ of the system.

Once ρ is determined for a particular magnetization orientation configuration, the GMR is obtained by finding the spin-dependent transmission $T_\sigma = \mathrm{Tr}\{[\mathrm{Im}(\Sigma^r_L)G^r\,\mathrm{Im}(\Sigma^r_R)G^a]_\sigma\}$. Here $G^{r(a)}$ is the retarded (advanced) Green's function for the device, while $\Sigma^r_{L(R)}$ is the self-energy which accounts for the semi-infinite left (right) lead.

This is the first *ab initio* evaluation of either GMR or CITs in a magnetoelectronic circuit that does not contain ferromagnetic elements. CITs in antiferromagnetic systems cannot be estimated on the basis of total spin conservation considerations because the antiferromagnet order does not carry a total spin. The CITs must be computed microscopically by finding the change in the local spin-dependent exchange-correlation potential on each site due to the presence of nonequilibrium, current-carrying electrons and summing over all sites assuming rigid antiferromagnetic order. Rigidity is maintained because the torques associated with short-distance-scale changes in relative spin orientation are very large compared to CITs. The CITs are significant experimentally because they compete only with much smaller anisotropy torques. This picture of current-induced torques, and its implementation in the NEGF formalism, is spelled out in more detail in Ref. 6.

The contribution of atom i to the CIT (per current) is

$$\frac{\vec{\Gamma}_i}{I} = \frac{\mu_B}{e}\frac{\int dk_\parallel \sum_{\alpha,\beta\in i}(\vec{\Delta}_{\alpha,\beta}\times\vec{s}_{\beta,\alpha})}{\sum_\sigma \int dk_\parallel T_\sigma(E_f)}. \tag{1}$$

In the above α and β refer to orbitals, so that the sum is over all orbitals α and β of atom i. $\vec{\Delta}_{i,\alpha}\cdot\vec{\tau}/2$ is the spin-dependent part of the exchange-correlation potential for orbital α on atomic site i; its magnitude is in effect the size of the spin splitting for this orbital and site. Here $\vec{\tau}$ is the vector of Pauli spin matrices. (The presence of more than one orbital on a site and the orbital dependence of the spin-splitting fields they produce is one of the important differences between more realistic models of transition metal magnetism and simple generic one-band toy models of ferromagnetism.) The orbital and site-dependent nonequilibrium spin density which appears in Eq. (1) is given by

$$\vec{s}_{\alpha,\beta} = \rho^{(\alpha,\beta)}_{tr}\vec{\tau}, \quad \alpha,\beta \in i. \tag{2}$$

Since the system we consider is metallic, we assume that the nonequilibrium quantities in which we are interested can be evaluated in linear response; specifically, for the nonequilibrium density matrix,

$$\rho_{tr} = G^r\,\mathrm{Im}(\Sigma^r_L)G^a. \tag{3}$$

with all quantities evaluated at the Fermi energy. The torque which acts on the staggered antiferromagnetic order parameter is the corresponding sum of the torques on individual atoms. Since the directions of the spin-dependent exchange-correlation fields alternate from site to site, current-induced transverse spin densities of the same sign give total torque contributions of the same sign.[4]

III. Cr/Au/Cr TRILAYERS

We study a circuit with semi-infinite antiferromagnetic Cr leads and a Au spacer. Cr has a bcc lattice structure with lattice constant 2.88 Å, while Au is fcc with a lattice constant of 4.08 Å. The interface between these materials has a fortuitous lattice matching of two-dimensional square nets when they are grown epitaxially along the [001] direction, and the Au lattice is rotated by 45° around the growth direction. In this configuration the bulk square net lattice constants differ by less than 0.2%. The lattice-matching strains for Au on a [001] Cr substrate are therefore quite small.

The antiferromagnetic state of bulk Cr has been studied extensively.[13] The origin of antiferromagnetism in Cr is nesting between electron jack and hole neck pieces of the paramagnetic Fermi surface.[14,15] The nesting vector **Q** defines the spin-density-wave (SDW) period which is nearly commensurate with the lattice with $Qa/2\pi=0.95$, where a is the lattice constant. In thin-film and multilayer structures, Cr can exhibit paramagnetism as well as commensurate and incommensurate SDW states, depending on the film thickness and on the adjacent materials.[16–20] There is evidence of antiferromagnetism in Cr thin films grown on Au substrates for coverages greater than 12 ML.[21] Density functional theory, within the LSDA, has been previously used to study bulk Cr in a commensurate SDW state[22] and can predict the magnitude of the exchange splitting, the magnetic moment, and the lattice constant. For this study, we restrict our attention to Cr with a commensurate spin-density-wave structure in which the body-center spins and cube-corner spins have opposite orientations. This magnetic structure is metastable in the absence of a bias voltage for our thin-film structures in the local spin-density approximation. All interfaces are perpendicular to the [001] direction.

For the GMR calculations discussed below we have used a double-ζ with polarization basis set for both Cr and Au, and have found excellent agreement with bulk band-structure and density-of-states calculations. For the calculation of current-induced torques, we have used a single-ζ with polarization basis set, which still retains good accuracy for bulk properties. For the calculation of the self-consistent equilibrium density matrix, contributions from 900 k points within the two-dimensional (2D) Brillouin zone have been summed. For the calculation of the conductance and current induced torques, 25 600 k points have been summed.

As a matter of convention, we define parallel (P) and antiparallel (AP) alignment below in terms of the alignment of the Cr spins in the two layers on opposite sides of the Au spacer. The inset of Fig. 1 shows the geometry and spin structure of the systems considered.

IV. RESULTS

Figure 1 illustrates the dependence of the GMR ratio [defined as $(I_P-I_{AP})/I_{AP}$] on spacer thickness. In the limit of no spacer, the GMR ratio is negative, implying larger conductances for an antiparallel configuration. This property is anticipated since the AP case at zero spacer thickness corresponds simply to ballistic conduction through bulk antiferromagnetic Cr with unit transmission coefficient for all channels, whereas the parallel configuration implies a kink in the Cr antiferromagnetic order parameter configuration which reduces the transmission. For all nonzero spacers we have studied, we find that the GMR ratio is positive. The nonzero GMR for antiferromagnetic systems is perhaps surprising at first sight; for example, a simple Julliere-type two-channel conductor model, in which MR is due to spin-dependent conductance in the bulk, would predict that the GMR ratio is zero for antiferromagnetic systems. For antiferromagnets, GMR is, in this sense, purely an interface effect; for ferromagnets GMR is only partly (but often mainly) an interface effect.

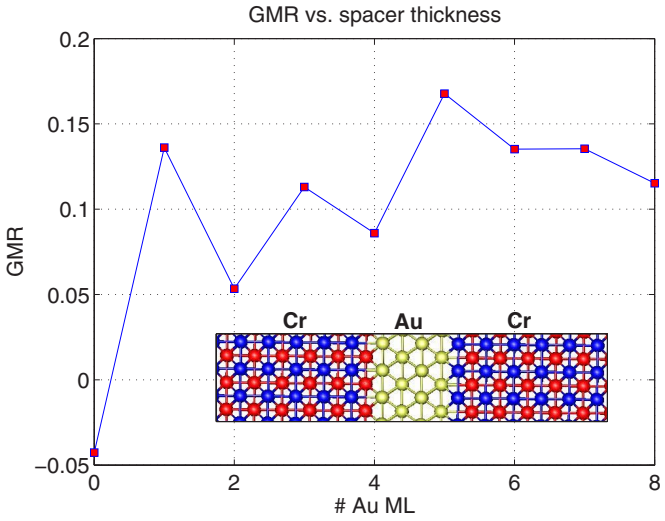

FIG. 1. (Color online) GMR as a function of spacer thickness. There is a sizable GMR for all spacer thicknesses. The inset shows the geometry for the four-layer spacer configuration—up and down spins are colored red and blue (light and dark), respectively. The configuration above illustrates an antiparallel configuration.

In the case of the previous toy model antiferromagnetic calculations,[4] GMR was due to phase coherent multiple scattering between two antiferromagnets. These effects are partially mitigated[7] at elevated temperatures by inelastic scattering which breaks phase coherence. The present *ab initio* calculations reveal a new contribution to antiferromagnetic GMR, explained below, which does not rely on phase coherence. The property that realistic antiferromagnets have GMR effects that are not dependent on phase coherence is encouraging from the point of view of potential applications, since it suggests larger robustness at elevated temperatures.

In order to identify the dominant GMR mechanism of Cr/Au/Cr trilayer systems, we have performed a separate NEGF calculation for a single interface between semi-infinite bulk Cr and semi-infinite bulk Au. The result is that there is a spin-dependent conductance with magnitude $(I_\uparrow-I_\downarrow)/(I_\uparrow+I_\downarrow)=-2.10\%$. The current is spin polarized in the direction opposite to the top layer of the antiferromagnet. For Cr/Au/Cr trilayers, this spin filtering implies that the conductance is maximum when the facing layers of the antiferromagnet have the same spin orientation; i.e., the P configuration has a higher conductance, even without any non local coherence effects. This effect is absent[4] in the single-band models that we studied earlier.

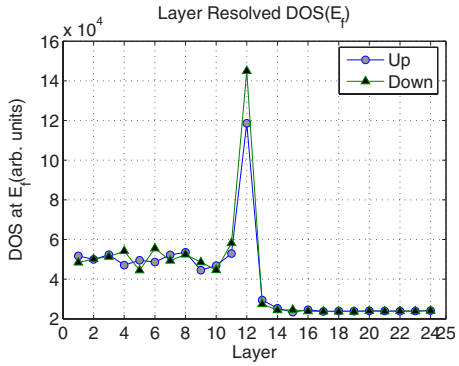

FIG. 2. (Color online) Layer- and spin-resolved density of states at the Fermi energy for a Cr-Au single interface system. Layers 1–12 are Cr, and 13–24 are Au. The pronounced enhancement of the density of states in layer 12 reflects the interface resonance. The spin polarization of the interface resonance is consistent with the fact that $T_{\downarrow} > T_{\uparrow}$ in the transport calculation.

To explore the origin of the spin-dependent interface resistance in greater detail, we have examined the layer- and $k_{\|}$-resolved local density of states (DOS) of the single-interface calculation (here $k_{\|}$ refers to the transverse momentum label). Figure 2 shows the layer-resolved results. (In the calculation, the first 12 layers on each side of the interface are allowed to differ from the bulk. In Fig. 2 layers 1–12 are the Cr layers in the scattering region near the interface while layers 13–24 are the Au layers in the scattering region.) We see that there is a pronounced interface resonance on the last Cr layer; this is a consequence of the difference between the Fermi surface topologies of Cr and Au. Moreover, this state is spin polarized, with direction opposite to that of the bulk local moment. Figure 3 shows the number of propagating channels in the Brillouin zone for Cr, which demonstrates that the Fermi surface of Cr differs strongly from the nearly spherical Fermi surface of Au. In particular, there are large regions in the Brillouin zone of Cr in which there is no propagating state, whereas Au has propagating states across all of the central region of the transverse Brillouin zone. Figure 4 shows the transverse wave-vector-resolved Fermi-level local density of states for layers 8, 10, 12 (the last Cr layer), and 16. Layer 8 is typical of bulk Cr, while layer 16 is typical of bulk Au. Layer 12, however, shows features of

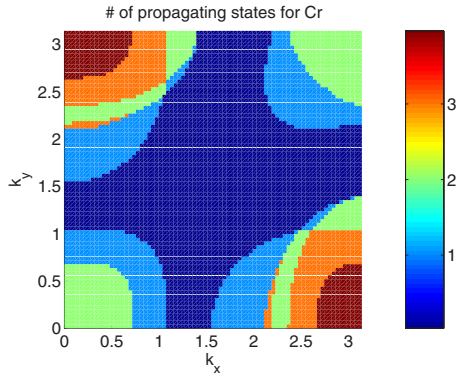

FIG. 3. (Color online) Number of propagating states in the [001] direction at the Fermi energy for bulk antiferromagnetic Cr.

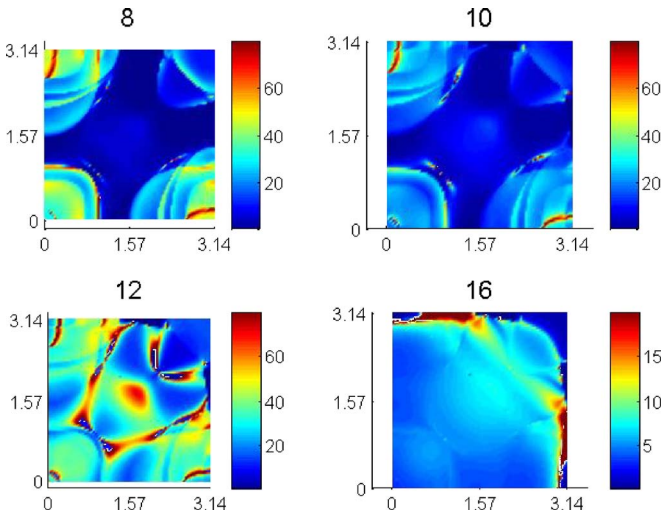

FIG. 4. (Color online) Transverse-momentum-resolved Fermi-energy density of states 8, 10, 12, and 16 of the single interface Cr-Au system. Layer 12 is the Cr layer closest to the interface. Layer 8 shows bulk Cr characteristics (compare to Fig. 3), while layer 16 shows bulk Au characteristics.

both materials; in particular, populations of states within the region of the Cr Brillouin zone with no propagating modes are responsible for the localized interface resonance. Figure 5 shows the total local density of states as a function of energy for layers near the interface. The rapid relaxation toward bulk values away from the interface is apparent. The interface layer has a highly distorted density of states function, a high density of states at the Fermi level, and a higher moment density which is responsible for a net ferromagnetic moment[10] contribution from the interface region. Apparently interruption of antiferromagnetic order both narrows the majority-spin bands and lowers the energy of minority spins in this interface layer. Hopping of down spins from the sub-interface layer on which they are the majority to the spacer layer is enhanced by the minority spin-interface resonance.

The enhanced moment density in the interface layer is accompanied by more attractive spin-up potentials on this layer and spin-dependent bonding across the Cr/Au interface. The effective hopping matrix elements across the interface have a spin-dependent contribution that is about 1% of their total values. In order to determine whether it is spin-dependent hopping or resonances related to spin-dependent site energies we have symmetrized hopping of the interface to remove its spin dependence and recalculated the conductance. We find the same value for the polarization, indicating that it is the interface resonance that is largely responsible for the polarization. The fact that the GMR is due to interface resonances, rather than to phase-coherent multiple-scattering across the spacer layer, suggests that the effect will be robust at elevated temperatures.

As mentioned earlier, the antiferromagnet/normal interface resistance is not spin dependent in the toy model systems previously studied.[4] The key property of the toy model which leads to this spin-independent interface resistance is that each antiferromagnetic unit cell is invariant under a combination of space and spin inversion. The *ab initio* mean-

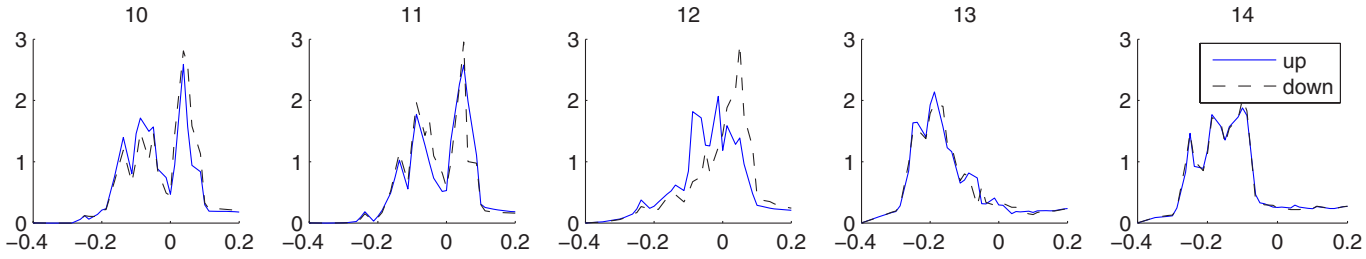

FIG. 5. (Color online) Density of states for layers 10–14 of the single interface Cr-Au system. The DOS relaxes to its bulk shape a couple of layers away from the interface. Layer 12 is the interface Cr layer, and the Fermi energy is 0.

field Hamiltonian does not have this property. A spin-dependent resistance will occur in the toy model when either the hopping amplitude from spacer to the top antiferromagnetic layer is made spin dependent or the exchange-splitting in the top layer is shifted from its bulk value. In this sense the interface resonance, while not directly responsible for transport, indirectly enables spin dependent transmission.

We have evaluated the current induced torques for a system with a four-Au-monolayer spacer. The angle between the staggered moments of the Cr leads was initialized to 90°: the staggered magnetization is along the $\hat{z}$ direction in the Cr layers to the left of the spacer and along the $-\hat{x}$ direction in the Cr layers to the right. A self-consistent noncollinear solution to the Kohn-Sham equations was obtained with this configuration. The resulting layer resolved torques, evaluated as described in Sec. II, are plotted in Fig. 6. For these data, electron flow is from-right to left lead. We find strong torques peaked in the first Cr layer, in contrast to the toy-model case in which the torques were constant in magnitude and alternated in direction from layer to layer.

For the torques in Fig. 6, the antiferromagnetic order parameters of the two layers would rotate together in a pinwheel fashion, much as in the case of standard spin torques in ferromagnets. If the right lead's order parameter were pinned in some fashion (for example, by exchange coupling the layer to a ferromagnet), then for electron flow from the right to left lead, the direction of the left lead's interfacial layer will tend to anti-align with that of the right lead's interfacial layer. This is consistent with a negative spin polarization induced by the interfacial resonance states found in the single-interface calculation.

To shed light on the origin of the new antiferromagnet current-induced-torque physics revealed by these *ab initio* calculations we focus on differences between the toy-model case, in which analytic calculations are possible, and the realistic Au/Cr case. Because the equilibrium torques that impose the antiferromagnetic (AFM) order will always be much stronger than the current-induced torques, we are mainly interested in the sum of the layer resolved torques which drives the antiferromagnetic order parameter and therefore competes only with anisotropy torques. The perfectly staggered torque obtained in the toy-model case arises from an out-of-plane current-induced spin density that is spatially constant within each antiferromagnet. (Here in-plane refers to the plane spanned by the orientations of the two antiferromagnetic layers and out-of-plane refers to the perpendicular direction, the y direction in our case.) The constant out-of-plane current-induced spin density in the toy model can be partially explained by the fact that Bloch wave vectors of up- and down-spin states are not spin split in antiferromagnets. It follows that a linear combination of transmitted up and down spins has a transverse spin density that is position independent [in contrast to the ferromagnetic case, in which the transverse spin density of a particular channel shows spatial oscillations with a period given by $(k_\uparrow - k_\downarrow)^{-1}$].[23] To see where this physics breaks down in our calculation, consider Fig. 3, which shows that a particular transverse channel has one to four possible values of k_z. For those channels with a single k_z value at the Fermi energy, we find that the contribution to the transverse spin density is spatially constant. Evidently the toy model does a good job of describing this type of transverse channel, suggesting that our earlier conclusion that there is a bulk contribution to the staggered spin torque in an antiferromagnet does have general validity. The present calculations emphasize, however, that there is also an interface contribution coming dominantly from channels with more than one k_z value at the Fermi energy. In this case the transmitted wave function is a

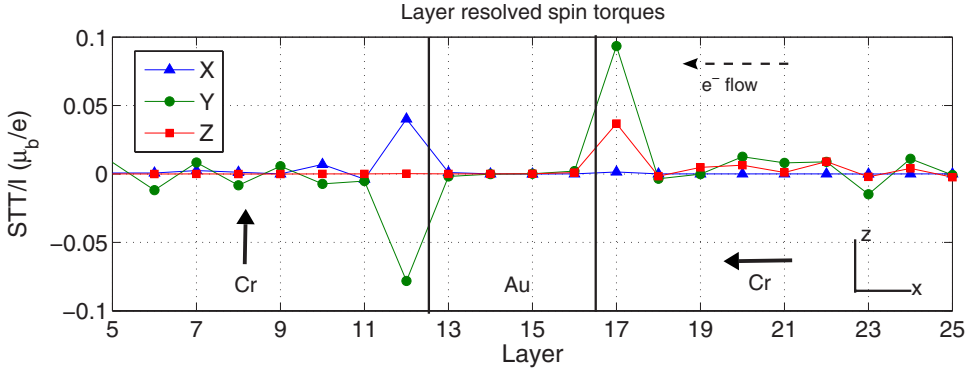

FIG. 6. (Color online) Layer-resolved current-induced torque per current. The (X,Y,Z) directions in the legend refer to the directions of the induced torques. The solid arrows in the figure refer to the orientation of the Cr interface spin. The torque is localized in the first layer of the Cr.

linear combination of states with different k_z values. These states interfere with each other to produce an oscillating transverse spin density. Summing over many channels with different oscillation periods of the transverse spin density leads to a rapid decay of the transverse spin density, exactly as in the case for ferromagnets.[23] A material with a simpler, single-valued Fermi surface would not have this interface contribution to the total staggered torque. The complex Fermi surface is necessary to stabilize the AFM order via nesting in the first place, however. In our case, the interface torque dominates the total staggered torque. It is nevertheless substantial, totalling $0.49\mu_B/e$.

To estimate the critical current for switching the antiferromagnetic order parameter, we take the anisotropy of bulk Cr with spins pointing along the $\mathbf{n}$ direction as $E(\mathbf{n}) = K_1(\hat{\mathbf{z}}\cdot\mathbf{n})^2 + 4K_2(\hat{\mathbf{x}}\cdot\mathbf{n})^2(\hat{\mathbf{y}}\cdot\mathbf{n})^2$, where[24] $K_1 = 10^3$ J m^{-3} and $K_2 = 10$ J m^{-3}, and take the magnetic damping parameter to be $\alpha = 0.1$.[24] Here K_1 is positive for $T > T_{sf} = 123.5$ K, and $\mathbf{Q}$, the spin density wave vector, is taken to be in the z direction. Near the fixed point $\mathbf{n} = \hat{\mathbf{x}}$, the damping torque per area is then $\Gamma = \alpha\gamma(K_1 + 4K_2)t$, where t is the thickness of the layer. (Note that antiferromagnets possess no demagnetizing field, so that the anisotropy does not include shape anisotropy and is due only to magnetocrystalline anisotropy.) The current required to have the current-induced torque overcome damping is therefore $0.049(\mu_b/e)\Gamma \approx 6.3 \times 10^{18} t$ (A/m^3). (In this we assume that the transfer torque efficiency calculated at $\theta = 90°$ is the same as that for small or large angle.) Typical values for critical current densities in ferromagnets are up to 100 times larger, primarily because of the large demagnetizing fields present in ferromagnets. We therefore expect that it will be possible to achieve current-induced switching in a circuit containing only antiferromagnetic elements.

V. SUMMARY AND CONCLUSIONS

In summary, we have performed a first-principles calculation of the nonequilibrium properties of Cr/Au/Cr trilayers. We have found that a system composed of Cr leads with an Au spacer possesses a robust GMR effect, which is due primarily to a spin-polarized interface state at the Au/Cr interface, and a strong current-induced torque which corresponds to a switching critical current more than an order of magnitude smaller than that of ferromagnets. These *ab initio* calculations demonstrate that current-induced torques in antiferromagnets have a bulk contribution from channels with only one band at the Fermi energy and an interface contribution, which is dominant in our case, from channels with more than one band at the Fermi energy. Our calculations demonstrate that all the basic effects of metal spintronics occur in circuits with only paramagnetic and antiferromagnetic elements.

The robust antiferromagnetic spintronics effects studied here occur in circuits in which current flows perpendicular to planes containing perfectly uncompensated spins. In realistic systems, structural disorder (interface roughness for example) or alloying will lead to a partial compensation of interfacial spins.[19,20,25–27] Recent studies of ultrathin Cr layers grown epitaxially on Au indicate typical terrace lengths from 20 to 100 nm.[28] The physical picture described in this work should be manifest for structures with lateral dimensions on the order or smaller than this length scale. For larger structures, averaging over domains at the interface may wash out the effects described here, with a reduction proportional to the area difference between spin-up and -down interfacial domains. The study of disorder at this magnetic domain length scale is not amenable to the *ab initio* approach adopted here; however, simpler models may be employed. The study of such effects is an important component to addressing the robustness and feasibility of antiferromagnetic spintronic effects.

It may be that initial studies of spin torques in antiferromagnetic systems will be easier to analyze in systems in which the antiferromagnets are exchange coupled to ferromagnets, whose orientation can be manipulated by external magnetic fields. There is, for example, already evidence[29] that current-induced torques act on the antiferromagnetic layer in spin-valve structures. Systems containing Cr antiferromagnetic films that are exchange coupled to Fe whiskers might also be attractive to study these kinds of current-induced torques since it is already known that weakly compensated Cr layers can be obtained relatively easily.[19,20,25] It may also be advantageous to consider Mn-doped Cr, as it is known to have a higher Néel temperature than pure Cr and forms a commensurate spin-density wave.[30] Although the materials challenges presented by antiferromagnetic metal spintronics are even stronger than those presented by ferromagnetic spintronics, we believe that the subject will prove interesting from both basic physics and potential application points of view.

ACKNOWLEDGMENTS

The authors acknowledge helpful interactions with Jack Bass, Sam Bader, Joseph Heller, Olle Heinonen, Chris Palmstrom, Stuart Parkin, Maxim Tsoi, and Z. Q. Qiu. This work was supported by the National Science Foundation under Grant No. DMR-0606489, by a grant from Seagate Corporation, and by the Welch Foundation. H.G. gratefully acknowledges financial support from NSERC of Canada, FRQNT of Quebec, and CIAR. A.S.N. was partially funded by Proyecto MECESUP FSM0204. Computational support was provided by the Texas Advanced Computing Center.

*Electronic address: haney411@physics.utexas.edu
†Electronic address: derek.waldron@mail.mcgill.ca
‡Electronic address: duine@phys.uu.nl
§Electronic address: alvaro.nunez@ucv.cl
‖Electronic address: guo@physics.mcgill.ca
¶Electronic address: macd@physics.utexas.edu; URL: http://www.ph.utexas.edu/ haney411/paulh.html

[1] M. Mierzejewski and M. Maska, Phys. Rev. B **73**, 205103 (2006).
[2] J. Slonczewski, J. Magn. Magn. Mater. **159**, L1 (1996); L. Berger, Phys. Rev. B **54**, 9353 (1996); Y. B. Bazaliy, B. A. Jones, and S.-C. Zhang, *ibid.* **57**, R3213 (1998).
[3] E. B. Myers, D. C. Ralph, J. A. Katine, R. N. Louie, and R. A. Buhrman, Science **285**, 867 (1999); J. A. Katine, F. J. Albert, R. A. Buhrman, E. B. Myers, and D. C. Ralph, Phys. Rev. Lett. **84**, 3149 (2000).
[4] A. S. Núñez, R. A. Duine, P. Haney, and A. H. MacDonald, Phys. Rev. B **73**, 214426 (2006).
[5] A. S. Núñez and A. H. MacDonald, Solid State Commun. **139**, 31 (2006).
[6] P. Haney, D. Waldron, R. A. Duine, A. S. Núñez, H. Guo, and A. H. MacDonald, arXiv:cond-mat/0611534.
[7] R. A. Duine, P. M. Haney, A. S. Núñez, and A. H. MacDonald, Phys. Rev. B **75**, 014433 (2007).
[8] S. Datta, *Electronic Transport in Mesoscopic Systems* (Cambridge University Press, Cambridge, England, 1995); C. Caroli, R. Combescot, P. Nozieres, and D. Saint-James, J. Phys. C **5**, 21 (1972).
[9] G. Zajac, S. D. Bader, and R. J. Friddle, Phys. Rev. B **31**, 4947 (1985).
[10] C. L. Fu and A. J. Freeman, Phys. Rev. B **33**, 1611 (1986).
[11] C. L. Fu, A. J. Freeman, and T. Oguchi, Phys. Rev. Lett. **54**, 2700 (1986).
[12] J. Taylor, H. Guo, and J. Wang, Phys. Rev. B **63**, 245407 (2001); **63**, 121104(R) (2001).
[13] E. Fawcett, Rev. Mod. Phys. **60**, 209 (1988).
[14] W. M. Lomer, Proc. Phys. Soc. London **80**, 489 (1962).
[15] A. W. Overhauser, Phys. Rev. **128**, 1437 (1962).
[16] H. Zabel, J. Phys.: Condens. Matter **11**, 9303 (1999).
[17] E. E. Fullerton, J. L. Robertson, A. R. E. Prinsloo, H. L. Alberts, and S. D. Bader, Phys. Rev. Lett. **91**, 237201 (2003).
[18] R. S. Fishman, J. Phys.: Condens. Matter **13**, R235 (2001).
[19] D. T. Pierce, J. Unguris, R. J. Celotta, and M. D. Stiles, J. Magn. Magn. Mater. **200**, 290 (1999).
[20] E. E. Fullerton, S. D. Bader, and J. L. Robertson, Phys. Rev. Lett. **77**, 1382 (1996).
[21] D. G. O'Neill and J. H. Weaver, Phys. Rev. B **37**, 8122 (1988).
[22] R. Hafner, D. Spišák, R. Lorenz, and J. Hafner, Phys. Rev. B **65**, 184432 (2002).
[23] M. D. Stiles and A. Zangwill, Phys. Rev. B **66**, 014407 (2002).
[24] E. W. Fenton, J. Phys. F: Met. Phys. **8**, 689 (1978).
[25] D. T. Pierce, Joseph A. Stroscio, J. Unguris, and R. J. Celotta, Phys. Rev. B **49**, 14564 (1994).
[26] R. Ravlic, M. Bode, A. Kubetzka, and R. Wiesendanger, Phys. Rev. B **67**, 174411 (2003).
[27] M. C. Hanf, C. Pirri, J. C. Peruchetti, D. Bolmont, and G. Gewinner, Phys. Rev. B **39**, 1546 (1989).
[28] T. Kawagoe, Y. Iguchi, A. Yamasaki, Y. Suzuki, K. Koike, and S. Suga, Phys. Rev. B **71**, 014427 (2005).
[29] Z. Wei, A. Sharma, A. S. Núñez, P. M. Haney, R. A. Duine, J. Bass, A. H. MacDonald, and M. Tsoi, Phys. Rev. Lett. **98**, 116603 (2007).
[30] E. Fawcett, H. L. Alberts, V. Yu Galkins, D. R. Noakes, and J. V. Yakhimi, Rev. Mod. Phys. **66**, 25 (1994).